Supporting Information

Bird et al. 10.1073/pnas.1002713107

SI Text

SI Methods. ***Peptide synthesis and characterization.*** All peptides used in this study were synthesized, purified, quantified, analyzed by circular dichroism (CD), and subjected to in vitro proteolysis testing as previously described (1). Peptides were produced on an Apex 396 (Aapptec) automated peptide synthesizer using Rink amide AM LL resin (EMD Biosciences, 0.2 mmol/g resin), at 50 μmol scale. The standard Fmoc protocol employed $2\times$ 10 min deprotections in 20% piperidine/NMP followed by a pair of consecutive methanol and dimethylformamide washes. The incorporated nonnatural amino acids were treated with 4×10 min incubations in 20% piperidine/NMP to achieve complete deprotection. Amino acid coupling was performed using 0.4 M stock solutions of Fmoc-protected amino acids, 0.67 M 2-(6-chloro-1H-benzotriazole-1-yl)-1,1,3,3-tetramethylaminium hexafluorophosphate, and 2 M N,N-diisopropyl ethylamine, yielding 1 mL of 0.2 M active ester (4 equivalents). Coupling frequency and incubation times were 2×30 min for standard residues, $2\times$ 45 min for the olefinic nonnatural amino acids, and 3×45 min for the residue following a nonnatural amino acid. For CD spectra, peptides were dissolved in 5 mM potassium phosphate (pH 7.5) or 10 mM HCl (pH 2) to a final concentration of 50 μM. Protease reaction samples contained 5 μL peptide in DMSO (1 mM stock) and 195 μL of buffer consisting of 50 mM phosphate buffer pH 7.4 with 2 mM $CaCl_2$ for chymotrypsin (0.5 ng/μL) or 10 mM HCl pH 2 for pepsin (0.5 ng/μL). Chymotryptic peptide fragments were analyzed by liquid chromatography/mass spectrometry (Agilent 1200).

NMR spectroscopy. Peptides were dissolved in 20% and 75% perdeuterated DMSO/H_2O (1–1.5 mM). One dimensional ^{1}H NMR spectra were obtained on a CMR E 600 MHz instrument (Massachusetts Institue of Technology/Harvard Magnetic Resonance Center) at 30 °C and 37 °C (WATERGATE pulse sequence, spectral width 10,000 Hz, 4096 complex data points collected over 128 scans, relaxation delay 3 s). NMR spectra were processed and analyzed with NMRPIPE (2) and iNMR (www.iNMR.net).

HIV infectivity assay. Single-round HIV-1 infectivity luciferase assays were performed using 293T human embryonic kidney and Cf2Th-CD4-CCR5 and Cf2Th-CD4-CXCR4 canine thymocytes as previously described (3). Cf2Th-CD4-CCR5 cells were used for infections by viruses with the YU2 and A-MLV envelope glycoproteins, and Cf2Th-CD4-CXCR4 cells for infection by viruses with HXBc2 and AMLV envelope glycoproteins. On the day of infection, peptide (0–3 μM) was added to recombinant viruses (10,000 RT units) to a final volume of 50 μL and incubated at 37 °C for 30 min. The medium was subsequently removed from the target cells, the cells incubated with virus-peptide mixture for 48 h at 37 °C, the medium again removed, cells lysed with 30 μL of passive lysis buffer (Promega) and three freeze—thaw cycles, and then luciferase activity measured upon addition of 100 μL of luciferin buffer (15 mM $MgSO_4$, 15 mM KPO_4, pH 7.8, 1 mM ATP, and 1 mM dithiothreitol) and 50 μL of 1 mM D-luciferin potassium salt. Trimeris enfuvirtide, obtained from the NIH AIDS Research and Reference Reagent Program, was used as a positive control for the enfuvirtide peptide synthesized in our laboratory.

Native polyacrylamide gel electrophoresis (native PAGE) assay. Doubly mutant V38A/N42T and V38E/N42S HR1 peptides (HXBc2 gp41 residues 29–79) (4, 5) were incubated with the indicated FITC-labeled HR2 peptides (40 μM, 1:1) for 30 min at 37 °C. The peptide mixtures were then analyzed by native PAGE (6, 7) using 18% tris-glycine precast gels and native sample and running buffers (Invitrogen). Fluorescent bands were imaged with Gel Doc XR (BioRad) and subjected to densitometric analysis using Quantity One v4.5.2 software (BioRad). The fraction of FITC-HR2 peptide complexed to mutant HR1 peptide was calculated according to the following formula: complex/(complex+ free FITC-HR2 peptide).

Pharmacokinetic studies. Peptides were dissolved in sterile aqueous 5% dextrose (1 mg/mL) and administered to 8–10 wk old male C57BL/6 mice (Jackson Laboratory) by bolus tail vein injection (10 mg/kg) or oral gavage (10 and 20 mg/kg). Blood was collected by retroorbital puncture at 5, 30, 60, 120, and 240 min after intravenous dosing and at 30 min after oral dosing from 3 animals at each time point. Plasma was harvested after centrifugation (2,500× g, 5 min, 4 °C) and stored at −70 °C until assayed. Peptide concentrations in plasma were determined by reversed-phase high performance liquid chromatography with electrospray ionization mass spectrometric detection (8, 9). Study samples were assayed together with a series of 7 calibration standards of either peptide in plasma at concentrations ranging from 1.25 to 50.0 μg/mL, drug-free plasma assayed with and without addition of the internal standard (enfuvirtide), and 3 quality control samples (3.75, 15.0, and 45.0 μg/mL). Standard curves were constructed by plotting the analyte/internal standard chromatographic peak area ratio against the known drug concentration in each calibration standard. Linear least squares regression was performed with weighting in proportion to the reciprocal of the analyte concentration normalized to the number of calibration standards. Values of the slope and *y*-intercept of the best-fit line were used to calculate the drug concentration in study samples. Plasma concentration-time curves were analyzed by standard noncompartmental methods using WinNonlin Professional 5.0 software (Pharsight Corp.).

1. Bird GH, Bernal F, Pitter K, Walensky LD (2008) Synthesis and biophysical characterization of stabilized alpha-helices of BCL-2 domains. *Methods Enzymol* 446:369–386.
2. Delaglio F, et al. (1995) NMRPipe: A multidimensional spectral processing system based on UNIX pipes. *J Biomol NMR* 6:277–293.
3. Madani N, Hubicki AM, Perdigoto AL, Springer M, Sodroski J (2007) Inhibition of human immunodeficiency virus envelope glycoprotein-mediated single cell lysis by low-molecular-weight antagonists of viral entry. *J Virol* 81:532–538.
4. Dwyer JJ, et al. (2003) The hydrophobic pocket contributes to the structural stability of the N-terminal coiled coil of HIV gp41 but is not required for six-helix bundle formation. *Biochemistry* 42:4945–4953.
5. Dwyer JJ, et al. (2007) Design of helical, oligomeric HIV-1 fusion inhibitor peptides with potent activity against enfuvirtide-resistant virus. *Proc Natl Acad Sci USA* 104:12772–12777.
6. He Y, et al. (2008) Potent HIV fusion inhibitors against Enfuvirtide-resistant HIV-1 strains. *Proc Natl Acad Sci USA* 105:16332–16337.
7. Liu SW, Zhao Q, Jiang SB (2003) Determination of the HIV-1 gp41 fusogenic core conformation modeled by synthetic peptides: Applicable for identification of HIV-1 fusion inhibitors. *Peptides* 24:1303–1313.
8. Aristoteli LP, Molloy MP, Baker MS (2007) Evaluation of endogenous plasma peptide extraction methods for mass spectrometric biomarker discovery. *J Proteome Res* 6:571–581.
9. John H, Walden M, Schafer S, Genz S, Forssmann WG (2004) Analytical procedures for quantification of peptides in pharmaceutical research by liquid chromatography-mass spectrometry. *Anal Bioanal Chem* 378:883–897.

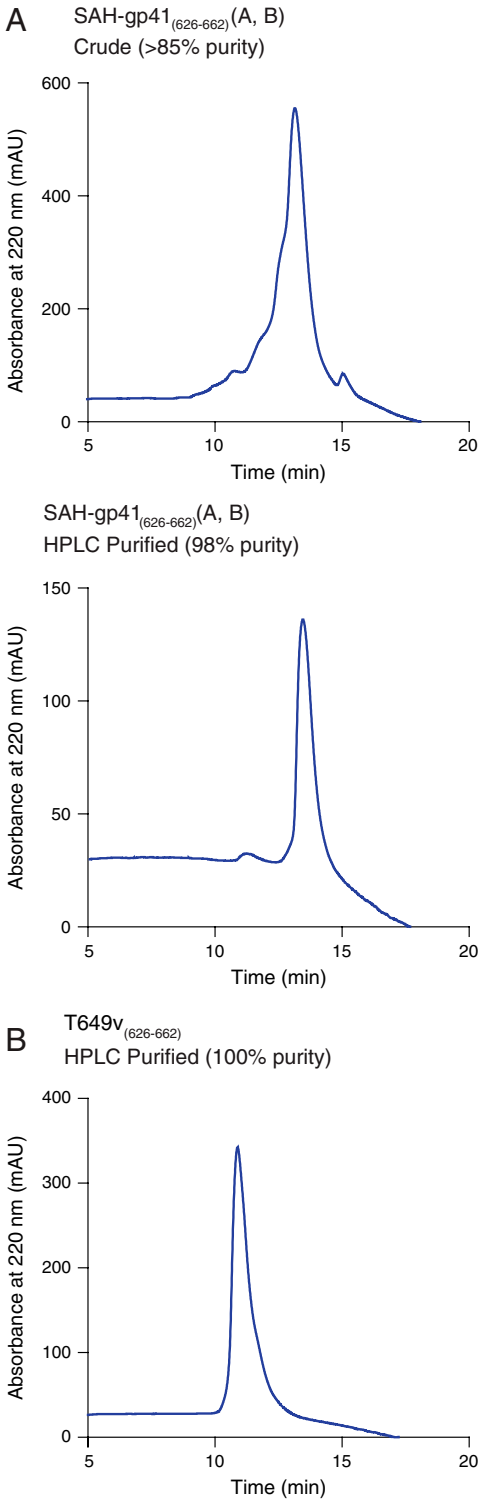

Fig. S1. Synthesis and purity of SAH-gp41$_{(626–662)}$(A, B). HPLC analysis of crude product from the automated peptide synthesis of SAH-gp41$_{(626–662)}$(A, B) revealed the desired full-length peptide as the predominant species at >85% purity even before HPLC purification. HPLC affords 98% pure product, which compares favorably with the purity of the corresponding unmodified peptide, T649v.

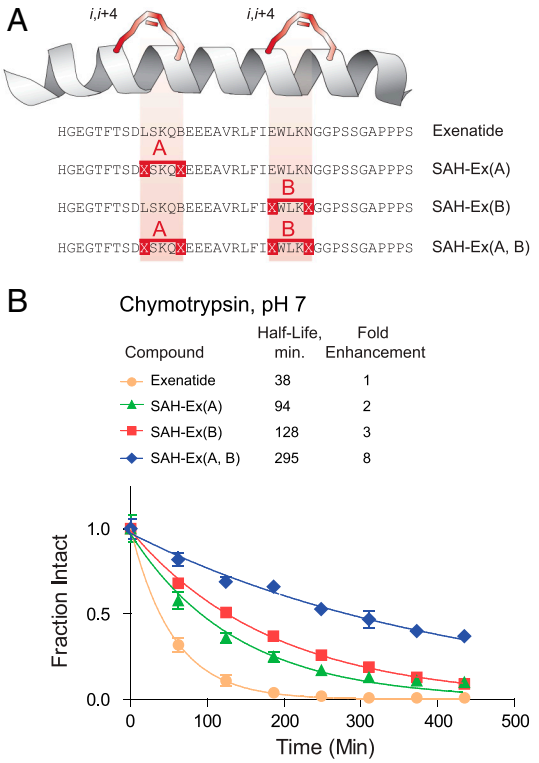

Fig. S2. Superior proteolytic resistance of a doubly stapled exenatide peptide. Like SAH-gp41 peptides, singly stapled exenatide derivatives show enhanced chymotrypsin resistance compared to the template peptide, and the doubly stapled peptide is more resistant than the unmodified and singly stapled peptides. X, substitution sites for crosslinking nonnatural amino acids; B, norleucine (substituted for methionine to optimize activity of the ruthenium catalyst). Fraction intact, mean ± s.d.

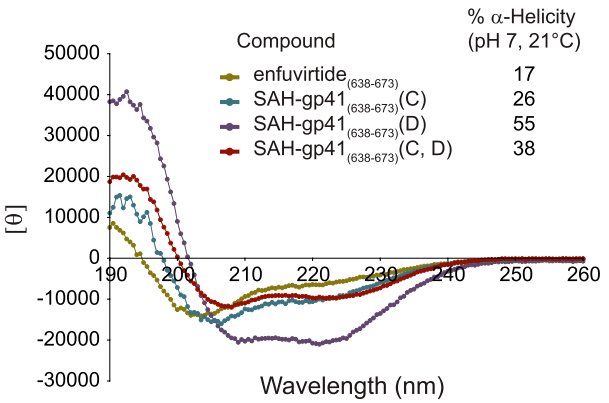

Fig. S3. Helical reinforcement of enfuvirtide by hydrocarbon stapling. Circular dichroism demonstrates that enfuvirtide is predominantly a random coil in solution, whereas SAH-gp41$_{(638–673)}$ peptides exhibit increased α-helical content. Like SAH-gp41$_{(626–662)}$(A, B), SAH-gp41$_{(638–673)}$(C, D), displays a percent α-helicity that lies in between that of the corresponding singly stapled peptides.

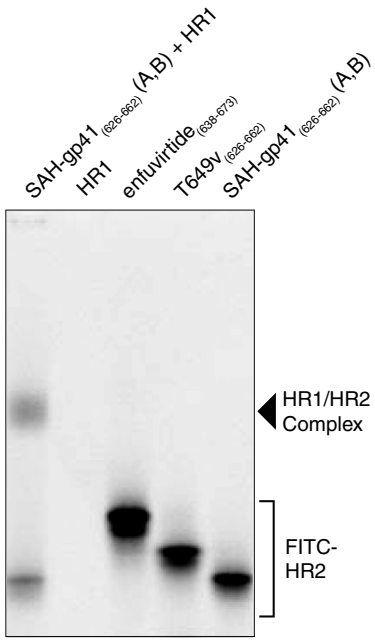

Fig. S4. Native gel electrophoresis of enfuvirtide, T649v, and SAH-gp41$_{(626–662)}$(A, B). Native PAGE analysis demonstrated that SAH-gp41$_{(626–662)}$(A, B) migrates as a monomeric species, with the doubly stapled peptide even running faster than the unmodified peptide standards (MW, approximately 4.9–5 kD). HR1/HR2 six-helix bundle standard (MW, approximately 33 kD).

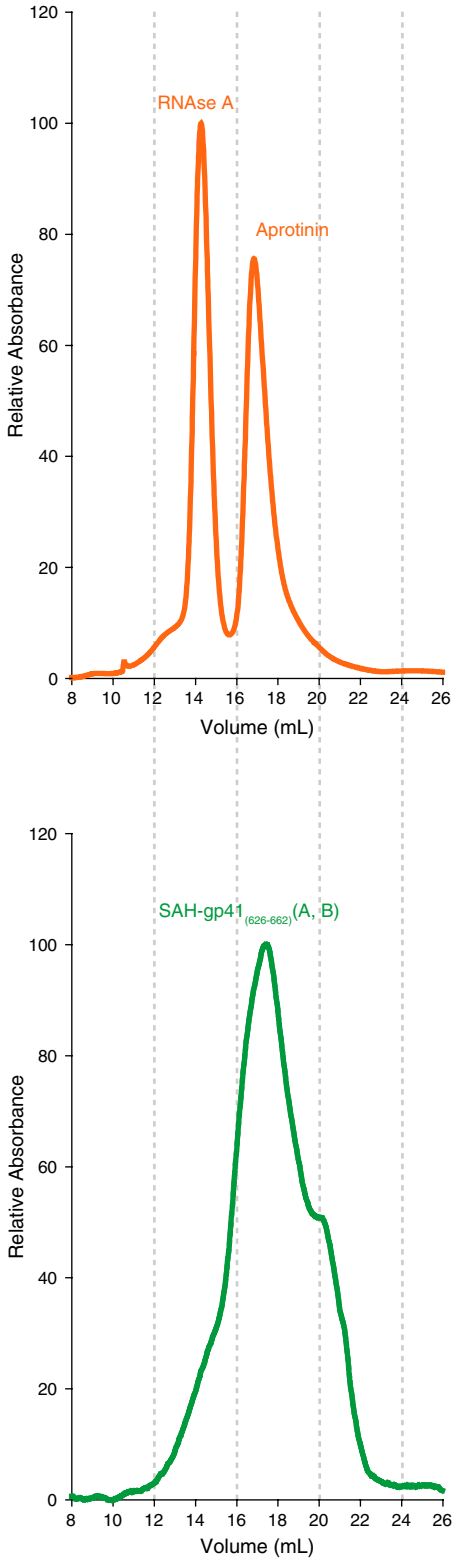

Fig. S5. Size-exclusion chromatography of SAH-gp41$_{(626–662)}$(A, B). The doubly stapled peptide elutes as a monomeric species by gel filtration analysis. Molecular weight standards, RNAse A (13.7 kD) and aprotinin (6.5 kD).

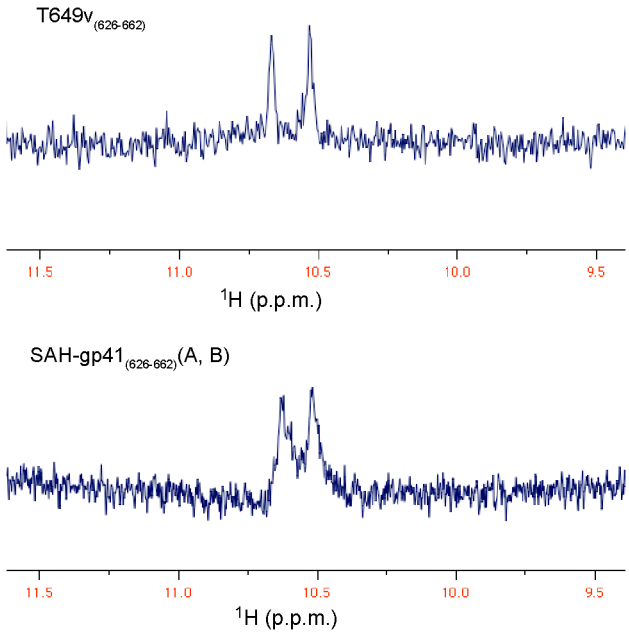

Fig. S6. Comparative ^{1}H NMR analysis of T649v and SAH-gp41$_{(626–662)}$(A, B). The indole protons (approximately 10.6 ppm) corresponding to the two N-terminal tryptophan residues of the T649v template peptide are represented by two sharp peaks in T649v, consistent with fast exchange between multiple conformations. In contrast, the indole proton peaks in the ^{1}H NMR spectrum of SAH-gp41$_{(626–662)}$(A, B) are broadened and split, reflective of a discretely structured N-terminus.

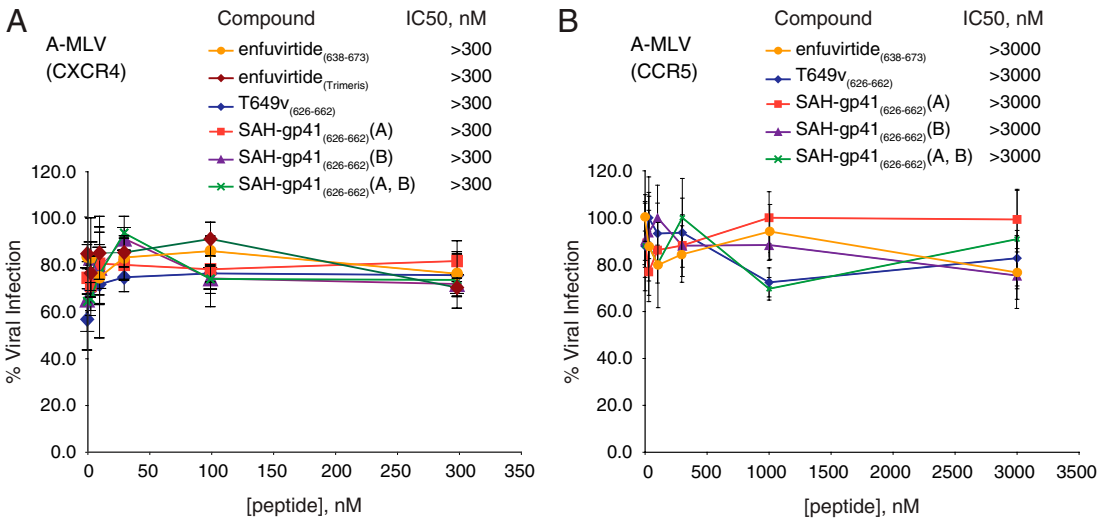

Fig. S7. Antiviral specificity of enfuvirtide and T649v-based peptides. (A, B) None of the peptides affected the infectivity of control virus bearing the A-MLV envelope glycoproteins. % viral infection, mean ± s.e.m.

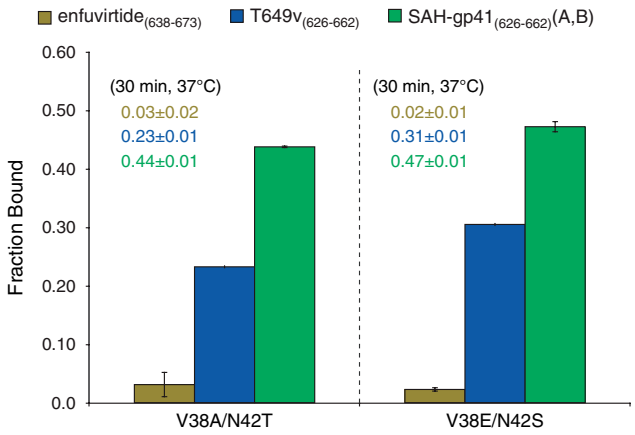

Fig. S8. Enhanced complex assembly of SAH-gp41$_{(626–662)}$(A, B) with doubly mutant HR1 peptides. Densitometric analyses of native PAGE fluorescence scans (Fig. 3 C and D) documented an up to 2-fold enhancement in binding activity of FITC-SAH-gp41$_{(626–662)}$(A, B) toward HR1 peptides bearing enfuvirtide resistance mutations, as compared to FITC-T649v. Fraction bound, mean ± s.e.m.

A Pepsin Cleavage Sites (predicted)

$_{626}$BTWBEWDREINNYTSLIHSLIEESQNQQEKNEQELLELDKWASLWNWF$_{673}$

		# Sites
BTWBEWDREINNYTSLIHSLIEESQNQQEKNEQELLE	T649v$_{(626-662)}$	10
BTWXEWDXEINNYTSLIHSLIEESQNQQEKNEQELLE	SAH-gp41$_{(626-662)}$(A)	10
BTWBEWDREINNYTSLIHSLIEESQNQXEKNXQELLE	SAH-gp41$_{(626-662)}$(B)	10
BTWXEWDXEINNYTSLIHSLIEESQNQXEKNXQELLE	SAH-gp41$_{(626-662)}$(A, B)	10
YTSLIHSLIEESQNQQEKNEQELLELDKWASLWNWF	enfuvirtide$_{(638-673)}$	14
YTXLIHXLIEESQNQQEKNEQELLELDKWASLWNWF	SAH-gp41$_{(638-673)}$(C)	14
YTSLIHSLIEESQNQQEKNEQELLELXKWAXLWNWF	SAH-gp41$_{(638-673)}$(D)	14
YTXLIHXLIEESQNQQEKNEQELLELXKWAXLWNWF	SAH-gp41$_{(638-673)}$(C, D)	14

B

Compound	Half-Life, min.	Fold Enhancement
T649v$_{(626-662)}$	11	1
SAH-gp41$_{(626-662)}$(A)	118	11
SAH-gp41$_{(626-662)}$(B)	129	12
SAH-gp41$_{(626-662)}$(A, B)	2040	192

C

Compound	Half-Life, min.	Fold Enhancement
enfuvirtide$_{(638-673)}$	4	1
SAH-gp41$_{(638-673)}$(C)	3	-
SAH-gp41$_{(638-673)}$(D)	227	61
SAH-gp41$_{(638-673)}$(C, D)	3324	892

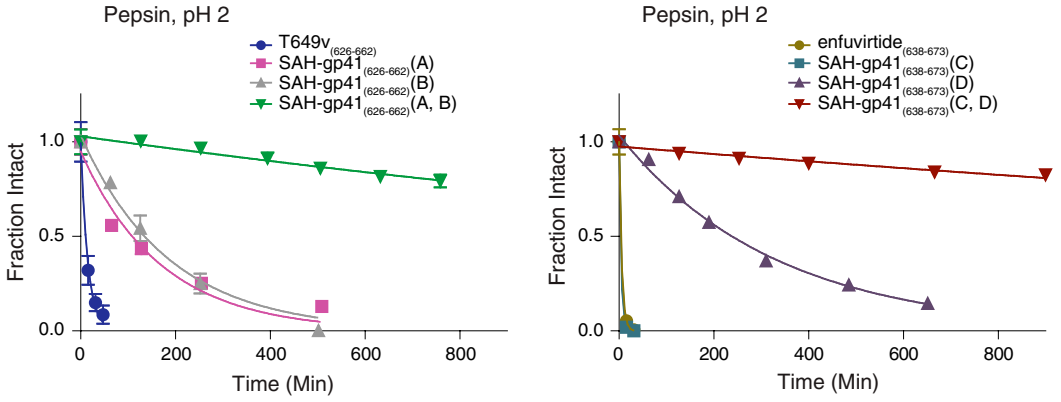

Fig. S9. Acid protease resistance of SAH-gp41 peptides. Upon exposure to pepsin, the doubly stapled SAH-gp41 peptides again demonstrate striking protease resistance compared to the corresponding unmodified and singly stapled peptides. The number of pepsin cleavage sites is unaffected by nonnatural amino acid substitution. Fraction intact, mean ± s.d.